DOI: 10.1002/ ((please add manuscript number))
Article type: Full Paper

Polarization-induced chirality in metamaterials via optomechanical interaction

Mingkai Liu, David A. Powell, Rui Guo, Ilya V. Shadrivov, Yuri S. Kivshar*

Dr. M. Liu, Dr. D. A. Powell, Mr. R. Guo, A/Prof. I. V. Shadrivov, Prof. Y. S. Kivshar
Nonlinear Physics Centre, Research School of Physics and Engineering, Australian National University, Canberra ACT 2601, Australia
E-mail: Mingkai.liu@anu.edu.au

Keywords: chiral, metamaterials, metasurfaces, optical forces, optomechanics

Abstract: A novel type of metamaterial is introduced, where the structural symmetry can be controlled by optical forces. Since symmetry sets fundamental bounds on the optical response, symmetry breaking changes the properties of metamaterials qualitatively over the entire resonant frequency band. This is achieved by a polarized pump beam, exerting optical forces which are not constrained by the structural symmetry. This new concept is illustrated for a metasurface composed of zig-zag chains of dipole meta-atoms, in which a highly asymmetric optical force exists for an appropriate incident polarization. The effect is employed to transform a planar achiral metasurface into a stereoscopic chiral structure. Importantly, the handedness of the induced chirality can be actively switched by changing the incident polarization. The proposed concept can be employed to achieve dynamic spatial control of metamaterials and metasurfaces at infrared and optical frequencies with subwavelength resolution.

1. Introduction

Metamaterials and metasurfaces provide a unique tool-kit to tailor the electromagnetic space and control the propagation of electromagnetic waves in unusual ways. The great design flexibility of these structures allows one to manipulate the amplitude, phase, and polarization of waves on demand. [1–8] In the design of metamaterials, structural symmetry sets fundamental bounds on the electromagnetic properties that can be achieved. For example, optical chiral effects, including circular dichroism and circular birefringence, typically require stereoscopic structures with broken mirror symmetry (three-dimensional chirality),[9–13] while circular conversion dichroism (elliptical dichroism) can be found in planar chiral geometries (two-dimensional chirality).[14–16]

Recently, much effort has been devoted to the development of *dynamically tunable metamaterials* (see References [17–24] and the references therein). Although the modulation of optical chiral effects is achieved by hybridizing chiral metamaterials with tunable media,[25, 26] the effects demonstrated are highly dispersive since they are based on resonance shifts. To arbitrarily manipulate the optical chiral effect, i.e. to not only control the strength but also the sign of chirality over the entire resonance band, one needs to dynamically and spatially control the *structural symmetry* at the *sub-wavelength* scale. This becomes challenging for metamaterial structures operating at infrared or optical frequencies, and introducing dielectrics to avoid the high losses of metals further increases the demands on the design.

One of the promising approaches for reconfiguring all-dielectric metamaterials and metasurfaces is to exploit *optomechanical effects*.[27– 32] As has been shown in the previous studies, the direction of an optical force acting on optomechanical structures is determined by the symmetry of the eigenmode profiles;[33–35] to generate an optical force acting in a certain direction, one needs to break the structural symmetry in that direction [28, 31, 36] – this is the case when the internal optical force of the system, originating from the near-field interaction within the system, dominates. However, in open systems like metamaterials, in addition to the internal force, there is also a non-negligible external force due to the interaction of incident light and the system, and the latter can be designed to be much stronger than the former. Importantly, since the external force has many degrees of freedom controlled by the incident wave, it provides a new possibility to generate an optical force and even to control its direction without the restrictions imposed by structural symmetry.

Here, we introduce an optomechanical paradigm that allows full spatial control of meta-materials and metasurfaces working at infrared and optical frequencies. First, we show analytically that for a general two-resonator coupled system, the optical forces acting on the two resonators are asymmetric as long as the incident field can simultaneously excite the two normal modes of the system, i.e. the symmetric and antisymmetric modes. We propose a simple system based on non-parallel coupled dipole meta-atoms, which is inherently achiral (mirror symmetric). We show analytically and numerically that due to the interaction and the collective enhancement in the array structure, the *external force* acting on the dipole meta-atoms can become highly asymmetric if the incident polarization *explicitly* breaks the mirror symmetry of the system, i.e. when it is not aligned with the symmetry axes of the system or becomes circularly polarized. This relative force is maximized around the antisymmetric mode, where the unusual phase response of the coupled meta-atoms leads to optical forces

acting in opposite directions. The effect can be employed to actuate the structure and transform it into a *stereoscopic chiral metamaterial*. Importantly, the induced optical activity is purely nonlinear, and the handedness of the nonlinear optical activity can be controlled with the polarization of the incident pump wave. By further introducing a spatial gradient in the incident polarization, one can generate chiral domains and spatially control the scattering of left and right circular polarizations. The proposed concept may pave the way towards *dynamic spatial modulation* of light with *subwavelength resolution.*

2. Results and Discussion

2.1. Analytical Modeling of Optical Forces in Coupled Pairs of Non-parallel Meta-atoms

To provide clear physical insight into this effect, we start with the simplest unit: a coupled pair of non-parallel electric meta-atoms, in which the effective dipole moments are aligned in the $x-y$ plane, as shown in **Figure 1**a. Although we use short metallic wires in our analytical model, there is no limitation on the actual implementation of the meta-atom as long as it behaves as a highly anisotropic dipole. The dipole meta-atoms have identical geometries but opposite orientation angles, and they form a coupled unit satisfying mirror symmetry. We define the two different orientations of meta-atoms with respect to the y-axis as $\theta_1 = -\theta_2 = \theta$. It will be subsequently shown that the effect in a one-dimensional or two-dimensional array is qualitatively the same and can be substantially enhanced due to collective resonances.

The key effect studied in this paper is the optical force acting on the dipole meta-atoms. For a meta-atom with induced charge and current distribution $\rho(\mathbf{r})$ and $\mathbf{J}(\mathbf{r})$ under external excitation, the total optical force acting on it can be calculated via $\mathbf{F}^{\text{opt}} = \int_V \rho\ (\mathbf{r})\mathbf{E}(\mathbf{r}) + \mathbf{J}\ (\mathbf{r}) \times \mathbf{B}(\mathbf{r})\ \mathrm{d}^3\mathbf{r}$, with $\mathbf{E}(\mathbf{r})$ and $\mathbf{B}(\mathbf{r})$ being the *total* electric and magnetic fields at the point $\mathbf{r}$, and the integral is performed over the volume of the meta-atom. Since the total field can be decomposed into two parts: the incident field $(\mathbf{E}^{\text{i}}, \mathbf{B}^{\text{i}})$ and the field scattered from the meta-atoms $(\mathbf{E}^{\text{s}}, \mathbf{B}^{\text{s}})$ in the coupled system, we decompose the total optical force according to these two contributing parts: $\mathbf{F}^{\text{opt}} = \mathbf{F}^{\text{ext}} + \mathbf{F}^{\text{int}}$. $\mathbf{F}^{\text{ext}}$ is the external force due to the interaction of the meta-atoms and the external incident field $(\mathbf{E}^{\text{i}}, \mathbf{B}^{\text{i}})$, and $\mathbf{F}^{\text{int}}$ is the internal force due to the near-field interaction of the meta-atoms via their scattered field $(\mathbf{E}^{\text{s}}, \mathbf{B}^{\text{s}})$. We are particularly interested in the z component of the time-averaged optical force. When the system is excited with a homogeneous plane wave, the forces can be determined from the following equations (see supplementary material for details):

$$\begin{aligned} F_z^{\text{ext}} &= \frac{1}{2}\mathrm{Re}\left[\int_V \mathrm{d}^3\mathbf{r}\ \rho^*(\mathbf{r})\mathbf{E}^{\text{i}}(\mathbf{r}) + \mathbf{J}^*(\mathbf{r}) \times \mathbf{B}^{\text{i}}(\mathbf{r})\right] \cdot \hat{\mathbf{e}}_z \\ &\approx \frac{k_z}{2}\mathrm{Im}\left[\mathbf{p} \cdot (\mathbf{E}^{\text{i}})^*\right], \end{aligned} \tag{1}$$

$$F_z^{\text{int}} = \frac{1}{2}\text{Re}\left[\int_V \text{d}^3\mathbf{r}\rho^*(\mathbf{r})\mathbf{E}^{\text{s}}(\mathbf{r}) + \mathbf{J}^*(\mathbf{r})\times\mathbf{B}^{\text{s}}(\mathbf{r})\right]\cdot\hat{\mathbf{e}}_z$$
$$= \frac{1}{2}\text{Re}\left\{\int_V\int_{V'}\text{d}^3\mathbf{r}'\text{d}^3\mathbf{r}\left(\frac{1}{|\mathbf{r}-\mathbf{r}'|}-\text{i}k\right)\frac{\exp(\text{i}k|\mathbf{r}-\mathbf{r}'|)}{4\pi\varepsilon|\mathbf{r}-\mathbf{r}'|}\right. \quad (2)$$
$$\left.\left[\rho^*(\mathbf{r})\rho(\mathbf{r}') - \frac{1}{c^2}\mathbf{J}^*(\mathbf{r})\cdot\mathbf{J}(\mathbf{r}')\right]\hat{\mathbf{e}}_{\mathbf{R}}\cdot\hat{\mathbf{e}}_z\right\}.$$

Here, $\mathbf{p} = \int_V d^3\mathbf{r}\rho(\mathbf{r})\,\mathbf{r}$ is the effective dipole moment of the meta-atom; k_z is the wave vector component along the z direction. F_z^{int} describes the internal force between two coupled meta-atoms, with their displacement vectors denoted by $\mathbf{r}$ and $\mathbf{r}'$, respectively; $\hat{\mathbf{e}}_{\mathbf{R}} = (\mathbf{r}-\mathbf{r}')/|\mathbf{r}-\mathbf{r}'|$. Note that Equation 1 is valid for homogeneous plane wave excitation, for a more general incident field, it can contain additional terms due to the local gradient of intensity $\nabla|\mathbf{E}^{\text{i}}|^2$ and the local curl of spin density $\nabla\times[\mathbf{E}^{\text{i}}\times(\mathbf{E}^{\text{i}})^*]$. [31]

Equations 1 and 2 show that while the direction of F_z^{int} is inherently bounded by the mode symmetry of the coupled system, the direction of F_z^{ext} is determined by the relative phase with respect to the incident field. For example, for a meta-atom in the coupled system, F_z^{int} changes sign when the coupled mode changes from symmetric to antisymmetric state [consider $\rho(\mathbf{r})\to-\rho(\mathbf{r})$ and $\mathbf{J}(\mathbf{r})\to-\mathbf{J}(\mathbf{r})$], and it vanishes when all the meta-atoms are on the same plane ($\hat{\mathbf{e}}_{\mathbf{R}}\cdot\hat{\mathbf{e}}_z = 0$). Thus it is *impossible* to actuate the originally planar structure in the z direction and transform it into a stereoscopic structure if only F_z^{int} is employed. In contrast, F_z^{ext} is free from such restriction, and the strength of F_z^{ext} can become much stronger in an array due to the collective enhancement (as shown below).

To model the electromagnetic interaction, we employ a semi-analytical model based on the free space Green's function (see supplementary material for details). [38–41] The coupled equations for a two-resonator system can be expressed explicitly as follows:

$$\text{i}\omega\begin{bmatrix} Z_{11} & Z_{12} \\ Z_{21} & Z_{22}\end{bmatrix}\begin{bmatrix} Q_1 \\ Q_2\end{bmatrix} = \begin{bmatrix} \mathcal{E}_1 \\ \mathcal{E}_2\end{bmatrix}, \quad (3)$$

where Q is the mode (charge) amplitude that describes the resonant behavior of meta-atoms. The impedance matrix describes the self and mutual interaction of the meta-atoms, in which Z_{ii} and Z_{ij} are the effective self-impedance and mutual impedance, respectively. All the matrix elements can be defined by the normalized current and charge distribution of the eigenmode of each individual meta-atom;[38-41] from symmetry we get $Z_{11} = Z_{22}, Z_{12} = Z_{21}$. $\mathcal{E}$ is the effective electromotive force imposed by the incident field; for plane wave excitation, $\mathcal{E} = \mathbf{l}\cdot\mathbf{E}^{\text{i}}$, where $\mathbf{l} = \mathbf{p}/Q$ is the normalized dipole moment of a single meta-atom.

Our two-resonator coupled system supports two normal modes: symmetric $\hat{\mathbf{e}}_{\text{S}} = \frac{1}{\sqrt{2}}[1,1]$ and antisymmetric $\hat{\mathbf{e}}_{\text{A}} = \frac{1}{\sqrt{2}}[1,-1]$. The coupled equations can be rewritten in a more instructive form in the basis of normal modes:

$$\mathrm{i}\omega\begin{bmatrix} Z_{\mathrm{S}} & 0 \\ 0 & Z_{\mathrm{A}} \end{bmatrix}\begin{bmatrix} Q_{\mathrm{S}} \\ Q_{\mathrm{A}} \end{bmatrix}=\begin{bmatrix} \mathcal{E}_{\mathrm{S}} \\ \mathcal{E}_{\mathrm{A}} \end{bmatrix}, \tag{4}$$

in which $Z_{\mathrm{S}}=Z_{ii}+Z_{ij}$, $Z_{\mathrm{A}}=Z_{ii}-Z_{ij}$ are the impedances of symmetric and antisymmetric modes, respectively; $Q_{\mathrm{S}}=(Q_1+Q_2)/\sqrt{2}$ and $Q_{\mathrm{A}}=(Q_1-Q_2)/\sqrt{2}$ are the corresponding normal mode amplitudes; $\mathcal{E}_{\mathrm{S}}=(\mathcal{E}_1+\mathcal{E}_2)/\sqrt{2}$ and $\mathcal{E}_{\mathrm{A}}=(\mathcal{E}_1-\mathcal{E}_2)/\sqrt{2}$ are the corresponding effective electromotive forces (see supplementary materials for details).

We assume that both meta-atoms are initially in the same plane, i.e. the separation of the two meta-atoms in the *z* direction is $s=r_{1,z}-r_{2,z}=0$. In this case, $F_z^{\mathrm{int}}=0$. From Equation 1, we get an explicit expression for the relative force

$$\Delta F_z=F_{1,z}-F_{2,z}=\frac{k_z}{2}\mathrm{Im}\left(Q_1\mathcal{E}_1^{*}-Q_2\mathcal{E}_2^{*}\right). \tag{5}$$

In the basis of normal modes, the relative force can be rewritten as

$$\Delta F_z=\frac{k_z}{4}\mathrm{Im}\left(Q_{\mathrm{S}}\mathcal{E}_{\mathrm{A}}^{*}+Q_{\mathrm{A}}\mathcal{E}_{\mathrm{S}}^{*}\right)=-\frac{k_z}{4\omega}\mathrm{Re}\left(\frac{\mathcal{E}_{\mathrm{S}}\mathcal{E}_{\mathrm{A}}^{*}}{Z_{\mathrm{S}}}+\frac{\mathcal{E}_{\mathrm{A}}\mathcal{E}_{\mathrm{S}}^{*}}{Z_{\mathrm{A}}}\right) \tag{6}$$

Equation 6 shows that in order to achieve a nonzero relative force, it is essential to have the incident field simultaneously excite both symmetric and antisymmetric modes so that neither $\mathcal{E}_{\mathrm{S}}$ nor $\mathcal{E}_{\mathrm{A}}$ vanishes. It should be noted that this conclusion is quite general since the model used from Equation 3 to Equation 6 is valid for any two-resonator coupled systems.

Now consider an incident plane wave propagating in the *x* - *z* plane:

$$\mathbf{E}^{\mathrm{i}}=\begin{pmatrix} E_x \\ E_y \\ E_z \end{pmatrix}=|\mathbf{E}^{\mathrm{i}}|\begin{pmatrix} \sin\psi\cos\alpha \\ e^{\mathrm{i}\varphi}\cos\psi \\ -\sin\psi\sin\alpha \end{pmatrix}e^{\mathrm{i}(-\omega t+k_z z+k_x x)} \tag{7}$$

where α is the angle of incidence (see Figure 1b), $k_z=k\cos\alpha$ and $k_x=k\sin\alpha$, ψ and φ describe the polarization state. At normal incidence, the relative force can be written in a concise form

$$\Delta F_z=-\frac{kl^2\,|\mathbf{E}^{\mathrm{i}}|\sin 2\theta\sin 2\psi}{2\omega}\mathrm{Re}\left(\frac{e^{-\mathrm{i}\varphi}}{Z_{\mathrm{S}}}+\frac{e^{\mathrm{i}\varphi}}{Z_{\mathrm{A}}}\right). \tag{8}$$

Equation 8 shows that for the non-degenerate configuration, i.e. $\theta\neq 0^{\circ}$ or 90°, the optical forces acting on the two meta-atoms can become asymmetric if the incident polarization explicitly breaks the system mirror symmetry, i.e. $\psi\neq 0^{\circ}$ or 90° [note that $\mathcal{E}_{\mathrm{A}}$ ($\mathcal{E}_{\mathrm{S}}$) becomes zero when $\psi=0^{\circ}$ (90°)]. Importantly, the sign of the relative force can be manipulated by the incident polarization state ψ and φ, and the optimum value of ψ is $\pm 45^{\circ}$ at normal incidence. The force asymmetry can be enhanced at the resonances of symmetric and anti-symmetric modes, and the enhancement factor is directly proportional to the quality factor of the resonance (as shown below). Note that while there are many ways to construct an anisotropic dipole meta-atom, the optimum design should provide the maximum normalized dipole moment *l*.

From energy conservation, it can be proved that for electric dipoles without material loss,

the square of the normalized dipole moment l is proportional to the real part of the self-impedance that represents the radiative loss

$$\mathrm{Re}(Z_{ii}) = \frac{k^3 l^2}{6\omega\pi\varepsilon} = \frac{k^2 l^2 \eta}{6\pi}, \tag{9}$$

where $\eta = \sqrt{\mu/\varepsilon}$ is the wave impedance of the environment. Substituting Equation 9 into Equation 8, we get

$$\Delta F_z = -\frac{3\pi |\mathbf{E}^{\mathrm{i}}|^2 \sin 2\theta \sin 2\psi}{\omega^2 \mu} \mathrm{Re}(Z_{ii}) \mathrm{Re}\left(\frac{e^{-\mathrm{i}\varphi}}{Z_{\mathrm{S}}} + \frac{e^{\mathrm{i}\varphi}}{Z_{\mathrm{A}}}\right). \tag{10}$$

Note that the factor $\mathrm{Re}(Z_{ii})\mathrm{Re}(e^{\mp\mathrm{i}\varphi}/Z_{\mathrm{S(A)}})$ represents the enhancement of the relative force, and for linearly polarized excitation ($\varphi = 0$), it reaches the maximum value of $\mathrm{Re}(Z_{ii})/\mathrm{Re}(Z_{\mathrm{S(A)}})$ at the resonant frequencies of the normal modes. Therefore, the enhancement of the relative force is directly proportional to the ratio of the linewidths of the single dipole resonance and the coupled normal modes.

2.2 Collective enhancement in arrays

The force asymmetry can be significantly enhanced when such non-parallel coupled dipole pairs form a zig-zag array, as shown in Figure 1b. For simplicity, we start with a one-dimensional infinite periodic array, of which the coupled equations can be simplified to the same form as Equation 3 using the Bloch boundary condition:

$$Q_{(i,n)} = Q_{(i,0)} e^{\mathrm{i}k_x n A_x} = Q_i e^{\mathrm{i}k_x n A_x}. \tag{11}$$

Here the subscript i = 1 or 2, denoting the two types of meta-atoms with different orientations, and n denotes the n_{th} meta-atom of type "i"; A_x is the lattice constant in the x direction. The elements of the impedance matrix in Equation 3 for the infinite array are redefined as:

$$Z_{ii} = Z_{(i,0),(i,0)} + 2\sum_{n=1}^{\infty} Z_{(i,0),(i,n)} \cos(k_x n A_x), \tag{12}$$

$$Z_{ij} = 2\sum_{n=0}^{\infty} Z_{(i,0),(j\neq i,n)} \cos[k_x (n+1/2) A_x]. \tag{13}$$

Since the coupled equation for the infinite array has the same form as the coupled dimer, the analysis and the conclusion from Equation 3 to Equation 10 is qualitatively the same. The quantitative difference comes from the collective enhancement that leads to a higher quality factor of the resonance. By properly manipulating the incident polarization, it is possible to generate a highly asymmetric F_z^{ext} along the array, which can be employed to trigger the symmetry breaking in the z direction, as shown below. As noted above, such flexibility is highly desirable for the optomechanical manipulation of metamaterials, since it provides the possibility to generate the optical force in directions prohibited by the symmetry of the normal modes.

To show a particular example, we first use the semi-analytical model to calculate the optical force acting on an infinite chain of anisotropic meta-atoms; the forces shown in this paper are all normalized to an incident power density of 1 mW $\mu\mathrm{m}^{-2}$. For simplicity, the dipole meta-atoms are treated as thin current lines made from perfect electric conductors,

with a sinusoidal current distribution. The angles and the length of the dipoles, and the periodicity of the array are chosen as $\theta = 15^\circ$, 670 nm and 1000 nm, respectively. The accuracy of the semi-analytical model is confirmed by comparison with full-wave calculations based on the Maxwell stress tensor (see Figure S1 in the supplementary material for details). It should be noted that in practical implementation, the constituent material of the meta-atoms can be metal or dielectric, as long as the meta-atoms function as anisotropic dipoles. In both cases the effects are qualitatively the same, as will be shown in Section 2.4.

To maximize the relative force, we choose a 45° linear polarization with $\psi = 45^\circ, \varphi = 0$. **Figure 2**a and 2b show the spectra of the mode (charge) amplitudes and phases of meta-atoms "1"and "2". The asymmetric Fano lineshape in Figure 2a is due to the interference of the broad symmetric mode and the narrow antisymmetric mode. At the antisymmetric mode around 201 THz (see Figure 2b), the optical forces acting on meta-atoms "1" and "2" become highly asymmetric. One unique feature is that the optical force acting on meta-atoms "2" can become negative (see Figure 2c). In contrast to previous studies, the origin of this negative force is neither a strong gradient force [42] nor the excitation of high order multipole moments.[43, 44] It is due to the unusual phase response of the meta-atoms' charge around the antisymmetric mode. For a single electric dipole, its phase around the resonance should be within (0, π) due to causality and passivity, and therefore the imaginary part of Equation 1 is positive. However, when the meta-atoms are coupled and support the antisymmetric mode, the phase of one type of meta-atom can fall into (−π, 0) (see Figure 2b), leading to a negative force. As a comparison, we plot the optical forces when the incident polarization is along the x direction ($\psi = 90^\circ, \varphi = 0$). In this situation, only the antisymmetric mode is excited, and the forces are identical and positive (see curves marked with diamonds in Figure 2c).

At normal incidence, the strongest relative force exists at $|\psi| = 45^\circ$, while the phase φ provides an additional degree of freedom to modify the effect. Figure 2d depicts the relative force as a function of φ, with $\psi = 45^\circ$; the corresponding polarization states of the incident pump wave are plotted on the right axis. Since the antisymmetric mode dominates around 201 THz, the strongest effect exists when the incident polarization is close to linear (see the circles in Figure 2d), and the direction of the relative force reverses as φ varies by 180°. When the incident polarization changes from linear ($\varphi = 0, 180^\circ$) to circular ($\varphi = \pm 90^\circ$), the relative force drops from maximum to zero at the resonant frequency, which is consistent with the prediction from Equation 8. Due to the collective nature of the resonance, the resonant frequency can be red shifted by increasing the incident angle α, and the relative force becomes even stronger due to the enhanced quality factor of the resonance (see Figure 2e). The relative force can be further enhanced by reducing the orientation angle θ, which leads to a higher quality factor of the resonance; however, the relative force starts to decrease and vanishes when the orientation angle reduces to the degenerate configuration of $\theta = 0$.

2.3 Polarization-induced Chirality

The highly asymmetric optical force shown above provides a new opportunity to control the structural symmetry of metamaterials. By hybridizing these meta-atoms with flexible mechanical feedback, it is possible to achieve controllable symmetry breaking and optical chiral effects (see schematics of Figure 1b and 1c). As the meta-atoms "1" and "2" are driven towards opposite directions by the external force F_z^{ext}, the mirror symmetry of the system is

broken, and the initially planar metasurface becomes a stereoscopic chiral metamaterial. Meanwhile, the internal force F_z^{int} starts to exist once the meta-atoms are no longer in the same plane. **Figure 3**a and 3b depict the external force and internal force as a function of the mutual separation s with the incident polarization of pump wave as $\psi = 45^\circ, \varphi = 0$. Unlike previous studies where the internal force/torque dominates,[27, 28, 30, 32] the external force plays a major role in the current design. This is mainly due to the relatively large center-to-center distance between the neighboring meta-atoms, which reduces the strength of near-field interaction and the internal force.

The force induced in a finite array is quantitatively very similar. We calculate the optical force acting on an array consisting of 30 pairs of meta-atoms with the same incident polarization used in Figure 2c. At the resonant frequency of 201 THz, the optical force shows high uniformity along the array, and apart from edge effects it agrees well with the results of the infinite array (see the Figure 2c and Figure 3c for comparison).

To estimate the nonlinear optomechanical interaction, we introduce elastic mechanical feedback into each meta-atom, with a spring constant κ = 100 pN μm^{-1}. We assume that the meta-atoms are only allowed to move in the z direction. A rigorous calculation of the system can be performed by solving both the optical response and the mechanical response simultaneously in the time-domain. However, since the mechanical oscillation period in our system is much longer than the lifetime of the optical resonance ($10^5 \sim 10^6$ times longer), and the oscillation is highly damped, the optical force at each integration time step of the mechanical dynamics can be approximated with the stationary solution that only depends on the instantaneous positions of the meta-atoms. Under this approximation, the coupled dynamic equations can be written as:

$$\mathrm{i}\omega \sum_{j=1}^{2}\sum_{n=1}^{N} Z_{(i,m),(j,n)} Q_{(j,n)} = \mathcal{E}_{(i,m)}, \tag{14}$$

$$M\ \ddot{\mathbf{r}}_{(i,m)}^{(\mathrm{c})} + \Gamma \dot{\mathbf{r}}_{(i,m)}^{(\mathrm{c})} = F_{(i,m)}^{\text{opt}} + F_{(i,m)}^{\text{mech}}\,. \tag{15}$$

Here M is the mass of the meta-atom, Γ is the mechanical damping due to the viscosity of the environment, $\mathbf{r}^{(\mathrm{c})}$ is the center of mass of the meta-atom, and $F_{(i,m)}^{\text{mech}} = -\kappa \mathbf{r}_{(i,m)}^{(\mathrm{c})} \cdot \hat{\mathbf{e}}_z$ is the mechanical feedback force approximated with Hooke's law. Note that the electromagnetic and mechanical equations are coupled because the mutual impedance $Z_{(i,m),(j,n)}$, the mode amplitude $Q_{(i,m)}$ and the resulting optical force $F_{(i,m)}^{\text{opt}}$ are functions of the displacements of *all* the meta-atoms in the array, which in turn depend on the optical forces acting on them (see supplementary material for more details).

We focus on the stationary response of the system. As shown in Figure 3e, the final stable state agrees well with the input optical force, mainly due to the weak nonlinear response of the force to the displacement change. To evaluate the chiral optical effect, we illuminate the chiral structure shown in Figure 3e with an x-polarized *probe* wave at 201.1 THz, and decompose the scattered field of the probe signal on the plane of y = 0 into left and right circular polarizations. The modulation contrast of the scattered wave, defined as $C_{\mathrm{M}} = (|E_{LCP}|^2 - |E_{RCP}|^2)/(|E_{LCP}|^2 + |E_{RCP}|^2)$, clearly demonstrates that the induced chiral structure in Figure 3e can be defined as "right-handed" since it scatters right circularly polarized waves much more strongly (see Figure 3g).

Apart from uniform deformation, we can also generate spatially varying deformation by

introducing a spatial gradient in the incident polarization. As an example, Figure 3d depicts the spatially varying force along the array. The input polarization of the pump wave shown in the figure (green arrows) can be synthesized by interfering two coherent plane waves with left and right elliptical polarizations, of which the in-plane components are circularly polarized: $\mathbf{E}_\perp = E[(\hat{\mathbf{e}}_x + \mathrm{i}\hat{\mathbf{e}}_y)e^{-\mathrm{i}k_\perp x} + (\hat{\mathbf{e}}_x - \mathrm{i}\hat{\mathbf{e}}_y)e^{\mathrm{i}k_\perp x}] \propto [\hat{\mathbf{e}}_x \cos(k_\perp x) + \hat{\mathbf{e}}_y \sin(k_\perp x)]$. The final stable state of the system consists of chiral domains that allow effective spatial modulation of circular polarizations (see Figure 3f and 3h). Unlike the case in our previous study, where chiral domains are generated via spontaneous chiral symmetry breaking,[32] the method shown here is well controlled by the *explicit symmetry breaking* from the pump wave.

It should be noted that the spatial resolution of the optomechanical response of metasurfaces depends not only on the field pattern of the pump wave but also on the design of the meta-surface. Take our zig-zag array as an example, as shown in Figure 3d, although the distance required for the in-plane polarization (green arrows) to make a full turn, i.e. from 0 degree to 180 degrees and back to 0 degree, is $2\pi / k_x = \lambda / \sin\alpha$, the size of the chiral domain is actually $\pi / (2k_x) = \lambda / (4\sin\alpha)$. So the size of the domain can easily go below half-wavelength when the incident angles of the two interference pump waves are larger than 30 degrees. Therefore, the spatial resolution of the optomechanical response in metasurfaces can be pushed to below diffraction limit and only be limited by the mutual distance of meta-atoms. On the other hand, we remind that apart from far field response, meta-atoms can also be employed to control the near-field property, such as achieving subwavelength focusing. Therefore, a dynamic control of the subwavelength near-field pattern does not necessarily require the spatial modulation to be changed significantly within a subwavelength distance.

2.4 Proposed Implementation in Optics

To estimate the practicality of the concept, we propose an implementation combining the meta-atoms with flexible nano-beams.[45–47] We perform full-wave calculation (CST Microwave Studio) of the optical response of a two-dimensional infinite periodic array composed of silicon ($\varepsilon_{\mathrm{Si}}$ = 12.15) meta-atoms supported by silicon nitride ($\varepsilon_{\mathrm{Si_3N_4}}$ = 3.92) nano-beams, as shown in **Figure 4**a. The optical forces acting on the two types of meta-atom are calculated based on the Maxwell stress tensor. The sharp resonance around 201 THz corresponds to the antisymmetric mode of the coupled silicon meta-atoms (see Figure 4b). The calculation confirms that the effect in this all-dielectric metamaterial is qualitatively the same as the semi-analytical modeling of PEC cut-wires shown above. The optical forces acting on the two types of meta-atoms can become highly asymmetric (one experiences a positive force and the other experiences a negative force) when excited with an appropriate incident polarization. The relative force is quite significant when the wave is incident from the side of the nano-beams and can be up to eight times the net optical force acting on the whole unit cell. Both 45° linear polarization and circular polarization can generate a strong relative force (see Figure 4b), which can drive the meta-atoms towards opposite directions and transform the planar array into a stereoscopic chiral system, leading to a giant optical chiral response. The effect of circular dichroism in transmittance becomes prominent when the relative displacement of neighboring beams s = 40 nm (see Figure 4c).

To estimate the nonlinear response, we design the nano-beams to be 220 μm long and fixed

at both ends. The Young's modulus of silicon nitride is chosen as 150 GPa. We use the finite element method (CST Multiphysics Studio) to model the mechanical deformation of the beam under a given pressure. We further assume that each nano-beam supports 45 meta-atoms on the central part (see the schematic in Figure 4a), so the optical relative force only acts on the central 40 μm section. The relation between the displacement at the center of the nano-beam and the total applied force is linear for small deflection, and the effective spring constant is estimated based on Hooke's law as $\kappa \approx 90$ pN μm^{-1}.

The relative displacement-dependent optical force calculated in the periodic structure is employed to calculate the stable state of the system under different input pump power levels. As shown in Figure 4d, for a 45° linearly polarized incident wave, the nano-beams can show a relative displacement of more than 50 nm with a pump power density as low as 10 μW μm^{-2}, which corresponds to a total power consumption of around 16 mW over a 40 μm × 40 μm area of the metamaterial. The corresponding giant nonlinear optical activity is shown in Figure 4e; more than 70° of polarization angle change can be found at the frequency of 200.8 THz.

One important feature of our structure distinguished from previous studies is that we can control the handedness of the metamaterial directly using circularly polarized waves. For example, by pumping the metamaterial with a right circularly polarized wave, it becomes more transparent to right circular polarization and more opaque to the opposite handedness (see Figure 4f). Note that in the linear regime the system is purely achiral. The current design provides a unique paradigm to achieve *pure nonlinear optical activity with a controllable handedness* in the optical frequency regime. In comparison to the previous proposal,[48] the nonlinear optical activity achieved here is based on the change of structural symmetry rather than a resonance shift; therefore the strength of nonlinear optical activity is symmetric for both handednesses.

3. Conclusion

We have proposed a novel paradigm to achieve full spatial controls of metamaterials working at infrared and optical frequencies. We have found that optical forces may play a significant role in triggering the structural symmetry breaking. We have analytically and numerically investigated the force asymmetry in pairs and arrays based on non-parallel coupled dipoles, showing that this effect is quite general as long as the incident wave can simultaneously excite the two normal modes. The effect in an array becomes more significant due to the collective field enhancement, which can be used to achieve achiral-chiral phase transitions with a controllable handedness of light. While the examples presented here are focused on the manipulation of structural symmetry and optical chirality, the concept can also be employed to achieve other types of spatial modulation. Due to the subwavelength nature of metamaterials, the proposed paradigm holds a great potential to achieve dynamic spatial control of the near-field components of light.

Supporting Information

Supporting Information is available from the Wiley Online Library or from the author.

Acknowledgements
We are grateful to A/Prof. Duk-Yong Choi for the helpful discussions on the nano-beams. This project was funded by the Australian Research Council, through Discovery Project DP150103611.

Received: ((will be filled in by the editorial staff))
Revised: ((will be filled in by the editorial staff))
Published online: ((will be filled in by the editorial staff))

References

[1] J. B. Pendry, D. Schurig, D. R. Smith, *Science* **2006**, *312*, 1780–1782.

[2] N. Engheta, R. W. Ziolkowski, *Metamaterials: Physics and Engineering Explorations*, John Wiley & Sons, **2006**.

[3] W. Cai, V. M. Shalaev, *Optical Metamaterials*, Springer, **2010**.

[4] H. Chen, C. Chan, P. Sheng, *Nature Mater.* **2010**, *9*, 387–396.

[5] A. Poddubny, I. Iorsh, P. Belov, Y. Kivshar, *Nature Photon.* **2013**, *7*, 948–957.

[6] N. Yu, F. Capasso, *Nature Mater.* **2014**, *13*, 139–150.

[7] S. Liu, T. J. Cui, Q. Xu, D. Bao, L. Du, X. Wan, W. X. Tang, C. Ouyang, X. Y. Zhou, H. Yuan, et al., *Light: Science & Applications* **2016**, *5*, e16076.

[8] X. Wan, T. Y. Chen, Q. Zhang, J. Y. Yin, Z. Tao, L. Zhang, X. Q. Chen, Y. B. Li, T. J. Cui, *Advanced Optical Materials* **2016**, DOI: 10.1002/adom.201600111.

[9] J. B. Pendry, *Science* **2004**, *306*, 1353–1355.

[10] S Tretyakov, A Sihvola, L Jylhä, *Photon. Nanostruct. Fundam. Appl.* **2005**, *3*, 107–115.

[11] S. Zhang, Y.-S. Park, J. Li, X. Lu, W. Zhang, X. Zhang, *Phys. Rev. Lett.* **2009**, *102*, 023901.

[12] J. K. Gansel, M. Thiel, M. S. Rill, M. Decker, K. Bade, V. Saile, G. von Freymann, S. Linden, M. Wegener, *Science* **2009**, *325*, 1513–1515.

[13] V. K. Valev, J. J. Baumberg, C. Sibilia, T. Verbiest, *Adv. Mater.* **2013**, *25*, 2517–2534.

[14] E Plum, X.-X. Liu, V. Fedotov, Y Chen, D. Tsai, N. Zheludev, *Phys. Rev. Lett.* **2009**, *102*, 113902.

[15] S. V. Zhukovsky, A. V. Novitsky, V. M. Galynsky, *Opt. Lett.* **2009**, *34*, 1988–1990.

[16] E. Plum, V. Fedotov, N. Zheludev, *J. Opt.* **2011**, *13*, 024006.

[17] A. D. Boardman, V. V. Grimalsky, Y. S. Kivshar, S. V. Koshevaya, M. Lapine, N. M. Litchinitser, V. N. Malnev, M. Noginov, Y. G. Rapoport, V. M. Shalaev, *Laser & Photon. Rev.* **2011**, *5*, 287–307.

[19] N. I. Zheludev, Y. S. Kivshar, *Nature Mater.* **2012**, *11*, 917–924.

[20] M. Lapine, I. V. Shadrivov, Y. S. Kivshar, *Rev. Mod. Phys.* **2014**, *86*, 1093.

[21] J. P. Turpin, J. A. Bossard, K. L. Morgan, D. H. Werner, P. L. Werner, *International Journal of Antennas and Propagation* **2014**, *2014*, 429837.

[22] K. Fan, W. J. Padilla, *Materials Today* **2015**, *18*, 39–50.

[23] I. V. Shadrivov, M. Lapine, Y. S. Kivshar, *Nonlinear, Tunable and Active Metamaterials*, Springer, **2015**.

[24] N. I. Zheludev, E. Plum, *Nature Nanotech.* **2016**, *11*, 16–22.

[25] S. Zhang, J. Zhou, Y.-S. Park, J. Rho, R. Singh, S. Nam, K. Azad, H.-T. Chen, X. Yin, A. J. Taylor, et al., *Nature Comm.* **2012**, *3*, 942.

[26] J. Zhou, D. R. Chowdhury, R. Zhao, A. K. Azad, H.-T. Chen, C. M. Soukoulis, A. J. Taylor, J. F. OHara, *Phys. Rev. B* **2012**, *86*, 035448.

[27] M. Lapine, I. V. Shadrivov, D. A. Powell, Y. S. Kivshar, *Nature Mater.* **2012**, *11*, 30–33.

[28] M. Liu, Y. Sun, D. A. Powell, I. V. Shadrivov, M. Lapine, R.C. McPhedran, Y. S. Kivshar, *Phys. Rev. B* **2013**, *87*, 235126.

[29] A. P. Slobozhanyuk, M. Lapine, D. A. Powell, I. V. Shadrivov, Y. S. Kivshar, R. C. McPhedran, P. A. Belov, *Adv. Mater.* **2013**, *25*, 3409–3412.

[30] M Liu, D. Powell, I. Shadrivov, M Lapine, Y. S. Kivshar, *New J. Phys.* **2013**, *15*, 073036.

[31] J. Zhang, K. F. MacDonald, N. I. Zheludev, *Light: Sci. & Appl.* **2013**, *2*, e96.

[32] M. Liu, D. A. Powell, I. V. Shadrivov, M. Lapine, Y. S. Kivshar, *Nature Comm.* **2014**, *5*, 4441.

[33] T. J. Kippenberg, K. J. Vahala, *Opt. Express* **2007**, *15*, 17172–17205.

[34] T. J. Kippenberg, K. J. Vahala, *Science* **2008**, *321*, 1172–1176.

[35] M. Aspelmeyer, T. J. Kippenberg, F. Marquardt, *Rev. Mod. Phys.* **2014**, *86*, 1391.

[36] Y. Sun, T. P. White, A. A. Sukhorukov, *Opt. Lett.* **2012**, *37*, 785–787.

[37] S. Albaladejo, M. I. Marqués, M. Laroche, J. J. Sáenz, *Phys. Rev. Lett.* **2009**, *102*, 113602.

[38] D. A. Powell, M. Lapine, M. V. Gorkunov, I. V. Shadrivov, Y. S. Kivshar, *Phys. Rev. B* **2010**, *82*, 155128.

[39] D. A. Powell, K. Hannam, I. V. Shadrivov, Y. S. Kivshar, *Phys. Rev. B* **2011**, *83*, 235420.

[40] M. Liu, D. A. Powell, I. V. Shadrivov, Y. S. Kivshar, *Appl. Phys. Lett.* **2012**, *100*, 111114.

[41] D. A. Powell, *Phys. Rev. B* **2014**, *90*, 075108.

[42] H Liu, J. Ng, S. Wang, Z. Lin, Z. Hang, C. Chan, S. Zhu, *Phys. Rev. Lett.* **2011**, *106*, 087401.

[43] J. Chen, J. Ng, Z. Lin, C. Chan, *Nature Photon.* **2011**, *5*, 531–534.

[44] A. Dogariu, S. Sukhov, J. Sáenz, *Nature Photon.* **2013**, *7*, 24–27.

[45] J.-Y. Ou, E. Plum, L. Jiang, N. I. Zheludev, *Nano Lett.* **2011**, *11*, 2142–2144.

[46] J.-Y. Ou, E. Plum, J. Zhang, N. I. Zheludev, *Nature Nanotech.* **2013**, *8*, 252–255.

[47] J. Valente, J.-Y. Ou, E. Plum, I. J. Youngs, N. I. Zheludev, *Nature Comm.* **2015**, *6*, 7021.

[48] I. V. Shadrivov, *Applied Physics Letters* **2012**, *101*, 041911.

Figure 1. (a) Schematic of a pair of non-parallel coupled dipole meta-atoms, which are mirror symmetric with respect to the *y* axis. The optical forces acting on the dipole meta-atoms become different when the incident polarization is not aligned with the symmetry axes, leading to a nonzero transverse optical torque M^{opt}. The direction of the torque can be controlled with incident polarization. (b) Schematic of a zig-zag array of dipole meta-atoms. When excited with an appropriate incident polarization, the optical force acting on the meta-atoms becomes highly asymmetric near the resonant frequency of the antisymmetric mode. By introducing flexible mechanical feedback, the relative force can be employed to transform the planar achiral structure ($s = 0$) into a stereoscopic chiral metamaterial ($s \neq 0$). The definition of the two eigenmodes is shown in the inset. (c) The handedness of the optomechanically induced chirality, denoted by the chiral index ζ, can be controlled by the incident polarization.

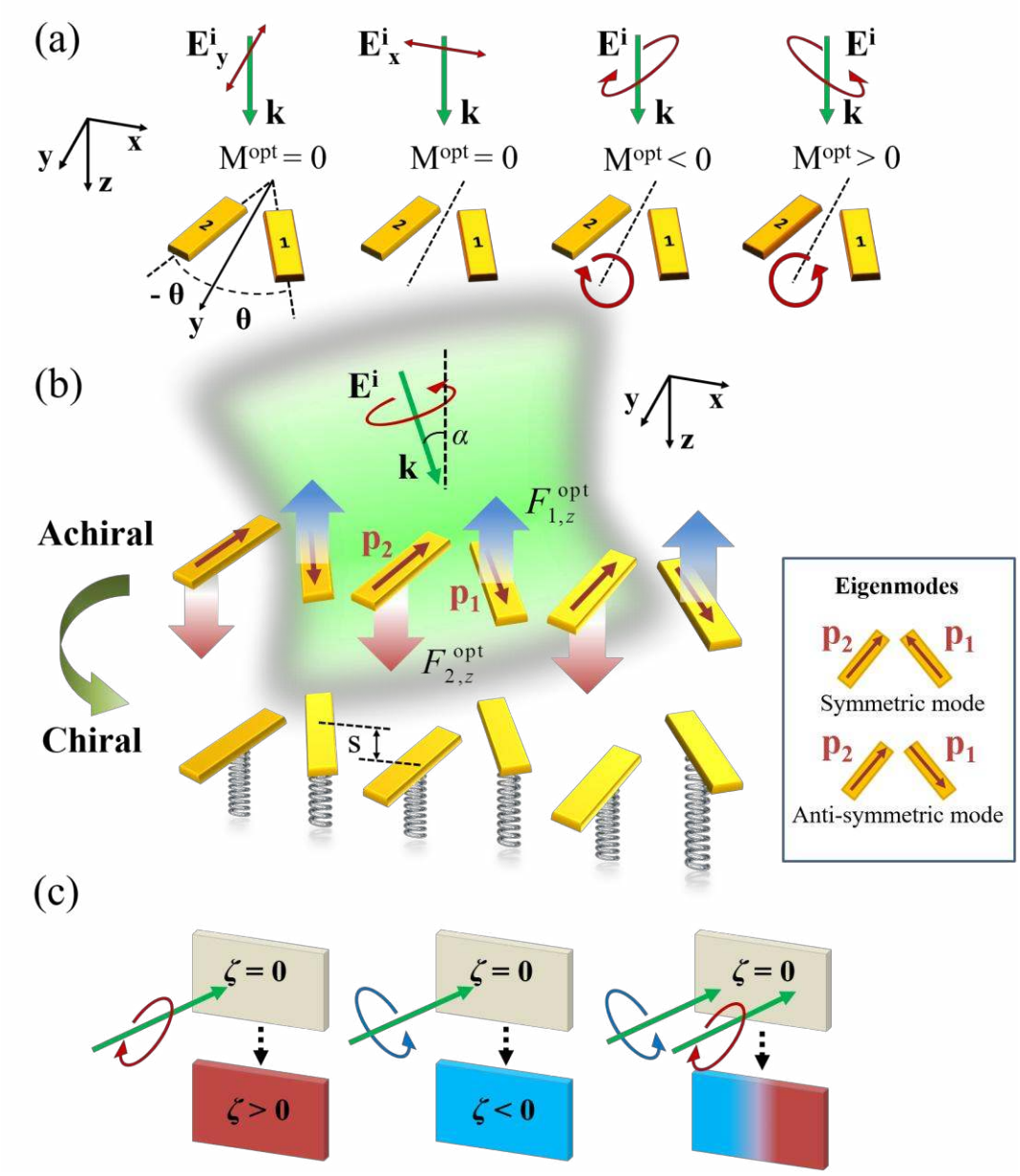

Figure 2. (a) The mode amplitudes, (b) the phases, and (c) the optical forces of the two types of meta-atom "1" and "2" in an infinite array. The incident polarization is $\psi = 45^\circ, \varphi = 0$ (45° linear polarization); the orientation angle $\theta = 15^\circ$. The dashed line indicates 201 THz. (d) The relative force ΔF_z as a function of φ, with $\psi = 45^\circ$; the black dotted lines indicate $\Delta F_z = 0$. For clarity, the corresponding polarization states are plotted on the right axis. (e) The relative force as a function of incident angle α, with $\psi = 45^\circ, \varphi = 0$. (f) The relative force ΔF_z for different orientation angle θ, with $\psi = 45^\circ, \varphi = 0$. All the plots except 2(e) are calculated under normal incidence ($\alpha = 0$).

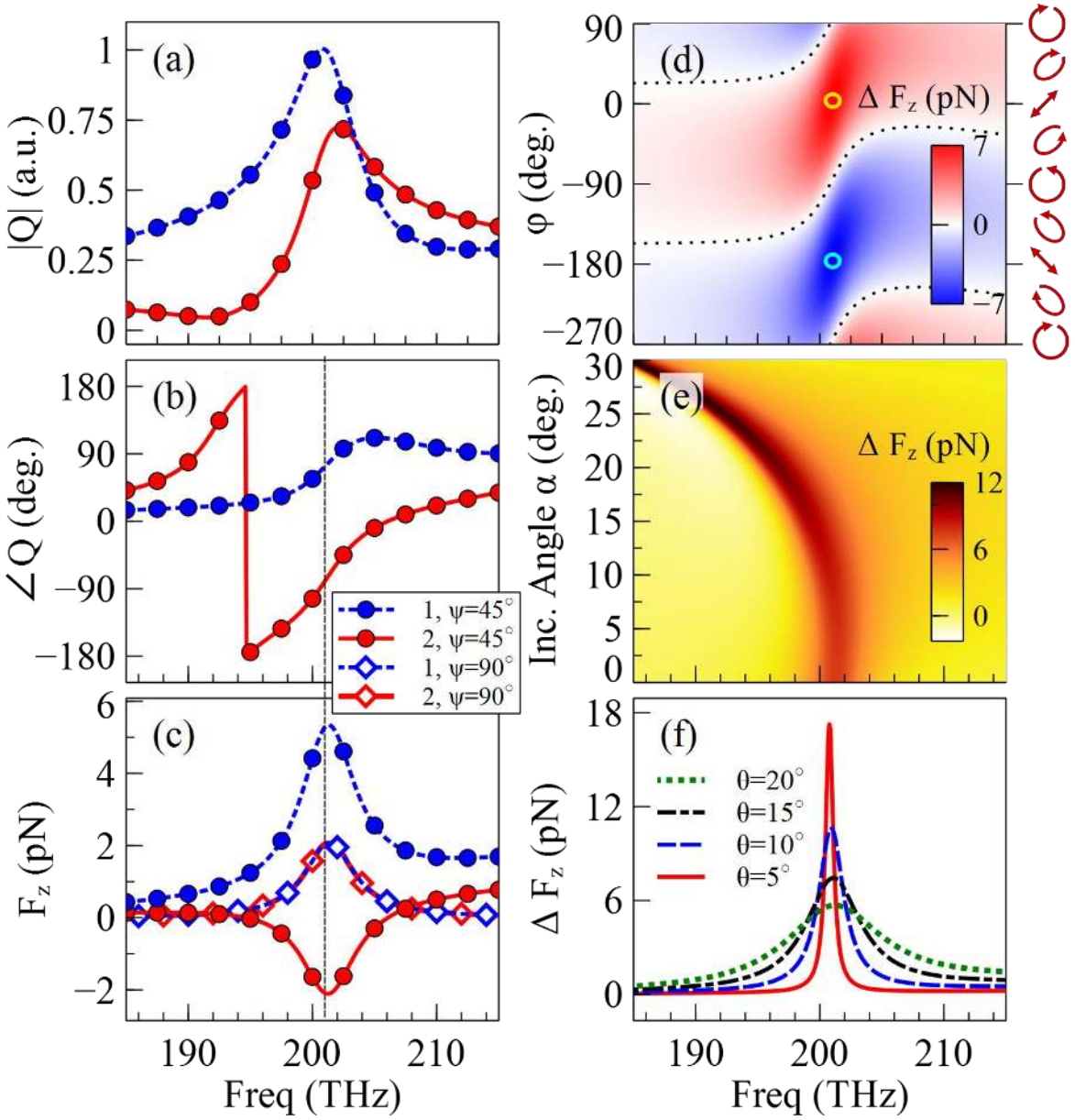

Figure 3. (a) and (b) The external force and the internal force acting on meta-atoms "1" and "2" in an infinite array under different separation *s* in the z direction, as denoted in Figure 1b. The incident frequency of the pump wave is 201 THz; the orientation angle $\theta = 15^{\circ}$; the incident polarization $\psi = 45^{\circ}, \varphi = 0$; the incident angle $\alpha = 0$. (c) and (d) The input optical force acting on a finite array. The blue circles and the red diamonds indicate meta-atoms "1" and "2". The green arrows show the spatial variation of the incident polarization on the $x - y$ plane. (e) and (f) The corresponding final stable displacement of the meta-atoms in the z direction. (g) and (h) The corresponding spatial distribution of the modulation contrast C_M of the scattered field in the plane of $y = 0$, generated by an *x*-polarized *probe* wave impinging on the chiral array and chiral domains shown in (e) and (f), respectively. The frequency of the probe wave is chosen as 201.1 THz.

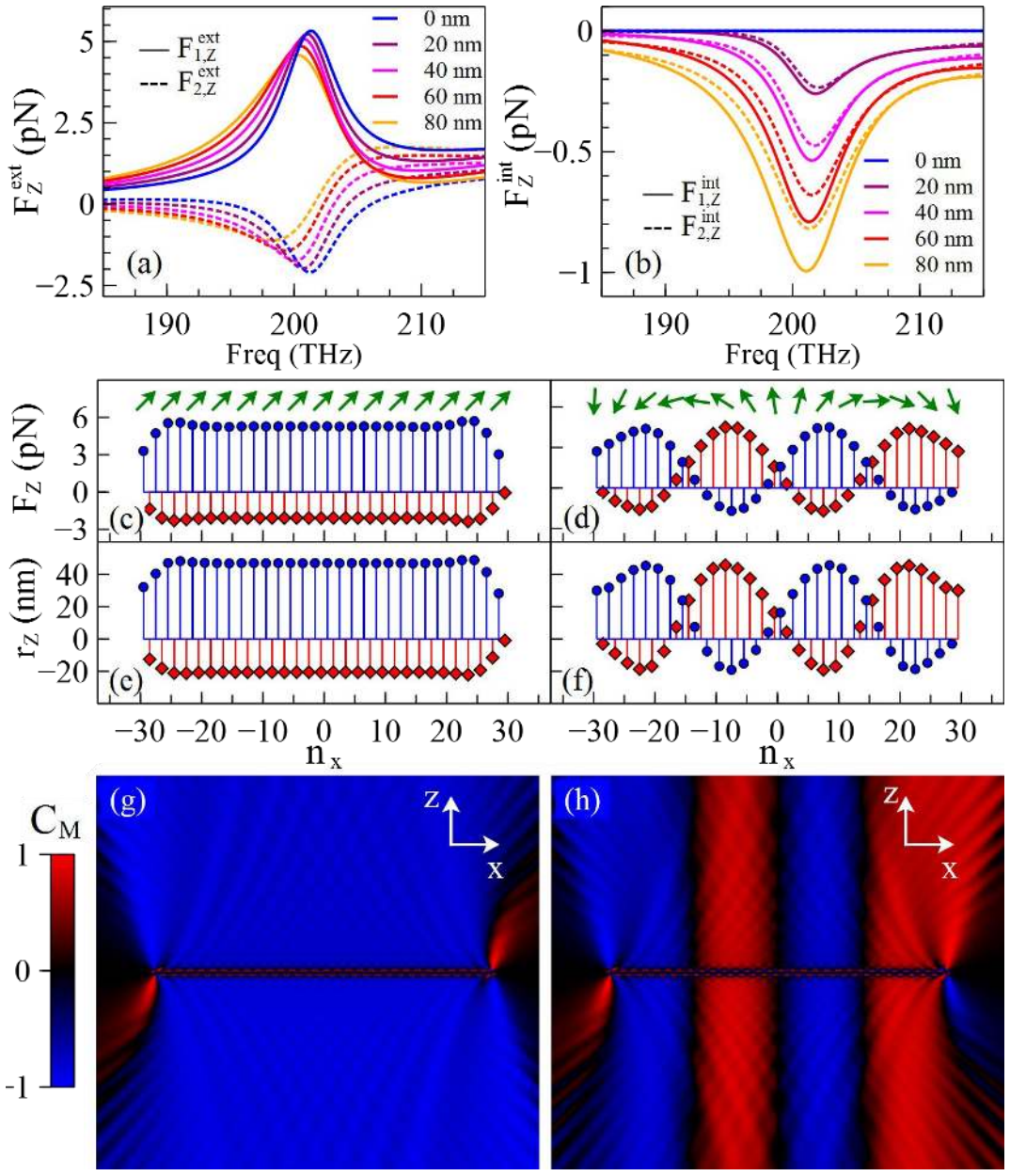

Figure 4. (a) Schematic of a metamaterial with silicon meta-atoms supported by silicon-nitride nano-beams. The lattice period in x and y directions is 1000 nm and 900 nm, respectively. The nano-beam width, thickness and the inter-beam gap are 400 nm, 100 nm, and 100 nm, respectively. The length, width, thickness and orientation angle of the meta-atoms are 550 nm, 220 nm, 150 nm, and ± 22.5° respectively. The deformation (exaggerated) of a pair of two-end-fixed nano-beams supporting meta-atoms "1" and "2" is also shown. (b) The relative force under linear and circular polarizations, and with different relative displacement s. (c) The circular dichroism under different relative displacement. (d) The relative displacement of nano-beams as a function of incident power density; the incident polarization is chosen as 45° linear polarization ($\psi = 45^\circ, \varphi = 0$). (e) The corresponding polarization angle of the transmitted wave. (f) Nonlinear circular dichroism of the metamaterial with right circularly polarized wave illumination. All the plots are calculated for pump wave at normal incidence.

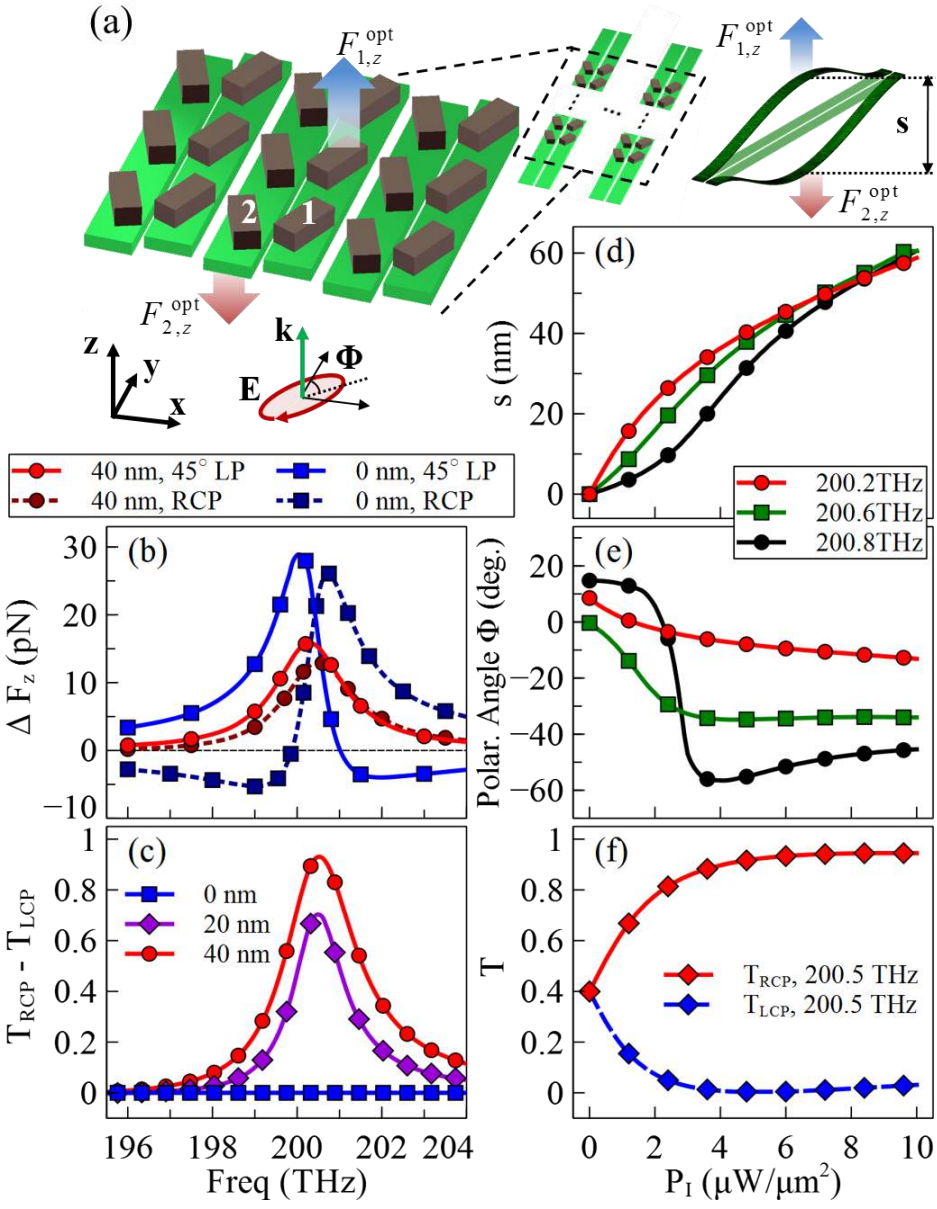

Keywords: chiral, metamaterials, metasurfaces, optical forces, optomechanics

Mingkai Liu*, David A. Powell, Rui Guo, Ilya V. Shadrivov, Yuri S. Kivshar

Title: Polarization-induced chirality in metamaterials via optomechanical interaction

The table of contents: Optomechanically-induced chirality, a novel mechanism to triger achiral-chiral phase transition in metamaterials is proposed and studied theoretically. This concept is illustrated for a specially-designed metasurface, in which the optical force acting on the meta-atoms becomes highly asymmetric for an appropriate incident polarization. The asymmetric force can transform the planar achiral metasurface into a stereoscopic chiral metamaterial with controllable handedness. (59 words)

ToC figure